Carcinogenesis, 2019, Vol. 40, No. 3, 403–411

doi:10.1093/carcin/bgz003
Advance Access publication April 10, 2019
Original Manuscript

ORIGINAL MANUSCRIPT

XPC protects against smoking- and carcinogen-induced lung adenocarcinoma

Huaxin Zhou[1], Jacob Saliba[1], George E.Sandusky[2] and Catherine R.Sears[1,3,*]

[1]Division of Pulmonary, Critical Care, Sleep and Occupational Medicine, Department of Medicine, and [2]Department of Pathology and Laboratory Medicine, Indiana University School of Medicine, Indianapolis, IN 46202, USA and [3]The Richard L. Roudebush Veterans Affairs Medical Center, Indianapolis, IN 46202, USA

*To whom correspondence should be addressed. Tel: +1 317 278 0413; Fax: +1 317 278 7030; Email: crufatto@iu.edu

Abstract

Cigarette smoke (CS) contains hundreds of carcinogens and is a potent inducer of oxidative and bulky DNA damage, which when insufficiently repaired leads to activation of DNA damage response and possibly mutations. The DNA repair protein xeroderma pigmentosum group C (XPC) is primed to play an important role in CS-induced DNA damage because of its function in initiating repair of both bulky oxidative DNA damage. We hypothesized that loss of XPC function will increase susceptibility to developing CS- and carcinogen-induced lung cancer through impaired repair of oxidative DNA damage. Mice deficient in XPC (XPC–/–) exposed to chronic CS developed lung tumors whereas their wild-type littermates (XPC+/+) did not. XPC–/– mice treated with the CS-carcinogen urethane developed lung adenocarcinomas representing progressive stages of tumor development, with lung tumor number increased 17-fold compared with XPC+/+ mice. Mice heterozygous for XPC (XPC+/–) demonstrated a gene–dose effect, developing an intermediate number of lung tumors with urethane treatment. Treatment of XPC–/– mice with the carcinogen 3-methylcholanthrene followed by the proliferative agent butylated hydroxytoluene resulted in a 2-fold increase in lung adenocarcinoma development. Finally, tumor number decreased 7-fold in the lungs of XPC–/– mice by concurrent treatment with the antioxidant, *N*-acetylcysteine. Altogether, this supports a mechanism by which decreased XPC expression promotes lung adenocarcinoma development in response to CS-carcinogen exposure, due in part to impaired oxidative DNA damage repair.

Introduction

Lung cancer is the leading cause of cancer deaths in the USA and Western European countries, and the number of lung cancers is increasing worldwide (1,2). Cigarette smoke (CS) is the primary exposure leading to the development of lung cancer, of which 85% are classified as non-small cell lung cancers (NSCLCs), with most prevalent histologic type being adenocarcinoma (3). The effects of CS on cell metabolism and function are many, but the primary carcinogenic CS effect is DNA damage. CS contains hundreds of carcinogens and direct exposure in the lung leads to a variety of DNA lesions, including bulky DNA adducts [such as polycyclic aromatic hydrocarbons (PAHs)] formed directly from carcinogens, oxidized DNA bases caused by CS-induced increases in oxidative stress, and single-strand and double-strand breaks caused by oxidative stress and/or repair intermediates (4,5). Although the connection between CS and lung cancer has been well established, less well understood is the mechanism by which CS-induced DNA lesions and DNA damage repair lead to lung cancer. Only 10–15% of smokers develop lung cancer, and it has been postulated that other exposures, epigenetic changes and/or genetic predisposition may be necessary in addition to CS exposure for lung cancer development (6). For instance, cigarette smokers with emphysema are at increased risk for lung cancer development compared with those without emphysema. This suggests that there may be a predisposing factor by which patients develop the seemingly disparate lung findings in emphysema (characterized by progressive loss of alveolar cells and structure) and lung cancer (characterized by unchecked cellular proliferation).

Received: June 5, 2018; **Revised:** December 21, 2018; **Accepted:** January 4, 2019

Abbreviations

AC	air control
BAL	bronchoalveolar lavage
BER	base excision repair
BHT	butylated hydroxytoluene
CS	cigarette smoke
CSE	CS extract
GG-NER	global genomic nucleotide excision repair
i.p.	intraperitoneal
MCA	3-methylcholanthrene
NAC	*N*-acetylcysteine
NSCLC	non-small cell lung cancer
PAH	polycyclic aromatic hydrocarbon
PBS	phosphate-buffered saline
WT	wild-type
XPC	xeroderma pigmentosum group C

Altered DNA repair capacity is considered a hallmark of cancer, leading to mutations and genomic instability (7). Decreased DNA repair capacity could be due to genetic predetermination or acquired in precancerous or cancerous lesions. In humans, decreased DNA repair capacity has been described as a risk factor for NSCLC development, and higher levels of DNA damage are observed in lung cancers (8), further supporting an important role for impaired DNA repair playing a critical role in lung cancer development.

The DNA repair protein, xeroderma pigmentosum group C (XPC), has a canonical role in the repair of bulky DNA damage, such as polycyclic aromatic hydrocarbons (PAHs), through global genomic nucleotide excision repair (GG-NER). Together with Rad23A/B and Centrin2, XPC initiates GG-NER through identification of DNA strand distortion from large, bulky DNA lesions throughout both transcribed and non-transcribed regions of the genome (9). An overlapping repair process, transcription-coupled NER, occurs when RNA polymerase II is stalled at bulky DNA lesions within actively transcribed regions of the genome. Downstream of the initial DNA damage recognition, these two NER pathways are identical (10). More recently, XPC has been implicated in repair of oxidative DNA lesions including 8-OHdG. Although the exact mechanism is yet to be fully elucidated, XPC recognition of the oxidative DNA lesion, 8-OHdG has been described *in vitro* and augmentation of base excision repair (BER) glycosylase activity of human 8-oxoguanine DNA glycosylase (hOgg1), and XPC augmentation of other BER proteins, Single-Strand-Selective Monofunctional Uracil-DNA Glycosylase 11 and thymidine-DNA glycosylase, have been described *in vitro* (11–14). In addition, increased oxidative DNA damage is observed in mice deficient in XPC when exposed to prooxidants *in vivo* (15). Given close associations between lung CS exposure, increased oxidative stress and associated DNA damage, this raises and intriguing possibility that XPC may be involved in repair of CS-induced DNA lesions through its role in GG-NER, BER of oxidative DNA damage or both.

A link between XPC deficiency and cancer development has been well established, as humans deficient in XPC develop melanomatous and non-melanomatous skin cancers early in life and at an increased number and severity when exposed to ultraviolet light. With these patients living longer by limiting sun exposure, XPC patients develop solid organ tumors at an increased incidence compared with the general population (16). In addition, epidemiologic studies suggest an association between common XPC polymorphisms and an increase in solid organ tumors, including lung cancers, although there is some debate regarding a link to CS exposure (17). Two XPC knockout mouse models exist, both of which develop characteristic skin cancers with exposure to ultraviolet light (13). XPC-deficient mice develop *de novo* precancerous and early cancerous lung tumors with advancing age (18). When exposed to oxidizing conditions, these mice were observed to show an increase in oxidative DNA damage and mutations in the liver compared with wild-type (WT) XPC mice (15). Mice deficient in xeroderma pigmentosum group A (XPA), which is essential for GG-NER and transcription-coupled NER, did not develop an increase in lung tumors with age compared with controls, suggesting that XPC may play a unique role in lung cancer development (19). More recently, we showed that XPC alters the DNA damage response to CS in lung epithelial cells *in vitro*, protecting cells from CS-induced extrinsic apoptosis and cell death, and protects against CS-induced emphysema in mouse models of CS exposure (20). However, it is not known how XPC affects development of CS- and carcinogen-induced lung cancer development.

Here we directly investigate the role of XPC in CS-induced lung cancers. We hypothesized that XPC deficiency would accelerate lung cancer development in mice exposed to chronic CS. Using a long-term CS exposure mode, we show that XPC-deficient mice are predisposed to development of precancerous and cancerous lung tumors compared with their WT littermates. Using two potent carcinogen models, we show that XPC knockout (XPC–/–) mice develop lung cancers of adenocarcinoma histologic type at an increased number compared with XPC WT (XPC+/+) littermates, with those mice heterozygous for XPC showing an intermediate number of tumors. Treatment with the antioxidant N-acetylcysteine (NAC) decreased urethane-induced tumor development, further supporting a role for XPC in repair of oxidative DNA damage. Altogether, this supports an important role of XPC in protecting against CS-induced lung cancer development.

Materials and methods

Chemicals

Urethane (ethyl carbamate), NAC, 3-methylcholanthrene (MCA) and butylated hydroxytoluene (BHT) were purchased from Sigma (St. Louis, MO). Other compounds and reagents purchased from Thermo Fisher Scientific (Waltham, MA), unless otherwise noted.

Animals

All mice experiments were conducted according to a Laboratory Animal Resource Center (LARC)-approved lab animal protocol. Mice heterozygous for XPC (mixed C57BL/6; 129 background) were purchased from Jackson Laboratories (Bar Harbor, ME), bred and genotyped as published previously (20). These mice had been back-crossed more than 10 generations prior to use. Littermate male and female mice, aged 6–8 weeks of age, were used for these experiments and maintained in accordance with institutional guidelines and approved by our local institutional animal care and use committee (IACUC) as published (20).

Mouse CS and carcinogen exposure models

For chronic CS exposure models, mice were exposed to reference cigarettes (3R4F; Tobacco Research Institute) for 5 h/day, 5 day/week via a TE-10 smoking device or ambient air (air control, AC) for the indicated durations as described previously (20). Chronic CS exposures were either 9 months continuous CS (or AC) or 5 months CS followed by 4 months AC (or 9 months AC) in XPC+/+ and XPC–/– mice, followed by necropsy. Experiments were performed in duplicate, total 18–20 mice per group. Mice (XPC+/+, XPC+/– and XPC–/–) received intraperitoneal (i.p.) injections of urethane at a dose of 1 g/kg body wt in phosphate-buffered saline (PBS) or vehicle (PBS) control weekly for 6 weeks and necropsy performed 26

weeks after initial urethane injection (21). Urethane mouse exposure experiments were performed in duplicate or triplicate for each treatment condition with animal numbers per group as detailed in Table 1. The MCA-BHT model was performed by i.p. injection of MCA in Mazola oil (15 mg/kg body wt) on week 1, followed by i.p. injection of BHT in Mazola oil (150 mg/kg body wt) on week 2 and subsequent i.p. injections of BHT in Mazola oil (200 mg/kg body wt) weekly on weeks 3–7, with necropsy performed 26 weeks after initial urethane injection (22). Experiments were performed in duplicate in XPC+/+ and XPC–/– mice, total of 12–16 per group. NAC was provided *ad libitum* in drinking water (~40 mM in water buffered to pH 7.4), changed three times a week (23). Lung harvest and bronchoalveolar lavage (BAL) were performed as described previously (20).

Tissue specimen collection and processing

All mice tissue samples were collected following a detailed LARC-approved lab animal protocol. In the histology study, lungs were fixed in 10% neutral buffered formalin at 4°C for 48 h following tissue processing and then embedded in paraffin. Four-micrometer sections were stained for routine hematoxylin and eosin staining or unstained for immunostaining.

Isolation and culture of Type 2 pneumocytes

Isolation of type 2 pneumocytes from mouse lungs was performed as previously described (24) with minor alterations. Briefly, mice were exsanguinated and perfused with sterile 0.9% saline solution. The trachea was cannulated, dispase (1 mg/ml in PBS, Worthington Biochemical) instilled followed by 1% low melting point agarose and solidification on ice for 2 min. Lungs were then removed and incubated in 2 ml dispase solution for 45 min with agitation (25°C). Lung tissue was teased apart from bronchi in a sterile petri dish containing 7 ml Dulbecco's modified Eagle's medium + 0.01% DNase I (Sigma). The cell suspension was incubated with red blood cell lysis buffer and filtered through sequentially smaller filters (70 μm, 40 μm) and nylon mesh (25 μm). Cells were labeled with biotinylated anti-CD45 and anti-CD16/32 antibodies, followed by incubation with magnetic streptavidin microbeads and negative selection through a magnetic-activated cell sorting microcolumn per manufacturer protocol (Miltenyi Biotec). These cells were plated on non-coated, tissue culture plates for 8 h, and the non-adherent cells collected and plated on fibronectin coated plates for additional experiments. Confirmation of type 2 pneumocytes by immunofluorescence microscopy staining using rabbit anti-mouse pro-SPC (AB3786, Millipore, 1:200) (25).

Comet assay

Assessment of DNA damage was performed by alkaline comet assay as published previously (26). Briefly, CS extract (CSE, 100%) was prepared by bubbling ambient air (AC) or smoke from two 3R4F cigarettes (CSE) into 20 ml PBS, adjusting the pH to 7.4, and passing through a 0.2 μm filter (20). Following 12 h of serum starvation, cells were cultured with AC or 5% CSE for 24 h. Cells are suspended in low-melting-point agarose and spread on prepared coverslips. Once solidified, the cells are lyzed and DNA unwound using an alkaline solution (2.5 M NaCl, 100 mM ethylenediaminetetraacetic acid, 10 mM Tris, 1% Triton X-100, pH 10) and single-cell electrophoresis performed according to manufacturer instructions (Trevigen). Slides were dehydrated in alcohol and stained with SYBR gold. Images were obtained at ×10 magnification (fluorescein isothiocyanate filter) using a Nikon Eclipse 90i microscope, captured by digital camera using NIS Elements. Analysis of ≥50 comets was determined using CometScore (TriTek). Mean tail DNA percentage from each of three independent experiments was compared using analysis of variance.

Immunostaining

The slides were deparaffinized in xylene and rehydrated using graded alcohols and water. Antigen retrieval was performed by immersing the slides by boiling in sodium citrate (pH 6.0) and endogenous peroxidase quenched with 3% hydrogen peroxide. Slides were blocked with in PBS-Tween 0.05% (Vector ABC Kit). Primary antibodies were diluted in Dako antibody diluent and biotinylated universal antibodies (Vector). Staining was performed using avidin–biotin complex horseradish peroxidase (ABC reagent, Vector) followed by diaminibenzidine substrate (Vector). A thorough washing was performed following each incubation. Counterstaining was performed using hematoxylin where indicated. The primary antibodies used for include the following: TTF1 (Abcam), 8-OHdG (N45.1, Abcam) and was performed as published previously (20).

Statistical analysis

Unless otherwise noted, statistical analysis was by analysis of variance using SigmaPlot (Systat Software) with statistical significance defined as $P < 0.05$.

Results

Deficiency in XPC promotes CS-induced lung adenocarcinoma

To evaluate the impact of XPC on smoking-induced lung cancer development, we exposed WT (XPC+/+) and XPC-deficient littermates (XPC–/–) aged 6–8 weeks, to chronic CS using a TE-10 smoking device (Figure 1A). Exposing these mice to 9 months chronic CS, we observed an increase in precancerous changes within the pulmonary epithelial cells in both XPC–/– and +/+ mice. The precancerous changes were more pronounced in XPC–/– mice, consisting of hyperplasia, atypia and dysplastic cells (Figure 1B). None of these mice developed frank lung tumors on both gross and microscopic examination. This was not surprising; although chronic CS exposure leads to lung cancer development in humans,

Table 1. Mouse tumor development and deaths according to genotype and treatment type.

Genotype	Treatment	Deaths	Mice with lung tumors (at time of planned necropsy)	Other findings
XPC+/+	PBS (control)	2/19[a] Females: 2/10	0/14	
XPC+/+	Urethane	3/22[a] Female: 0/11	12/19	Lymphoma
XPC+/–	PBS (control)	0/7	0/7	
XPC+/–	Urethane	1/19 Female: 1/10	17/18[b]	Ovarian mass (adenoma, TTF1 neg)
XPC–/–	PBS (control)	0/13	0/13	
XPC–/–	Urethane	1/35 Female: 0/19	34/34[b]	Lymphoma and thymic mass
XPC–/–	Urethane + NAC	5/18 Female: 5/11	12/13	Lymphoma

[a]One XPC+/+ PBS (control) and two XPC+/+ urethane-treated mice deaths because of complications of i.p. injection.
[b]Mice that died prior to harvest found to have multiple lung tumors.

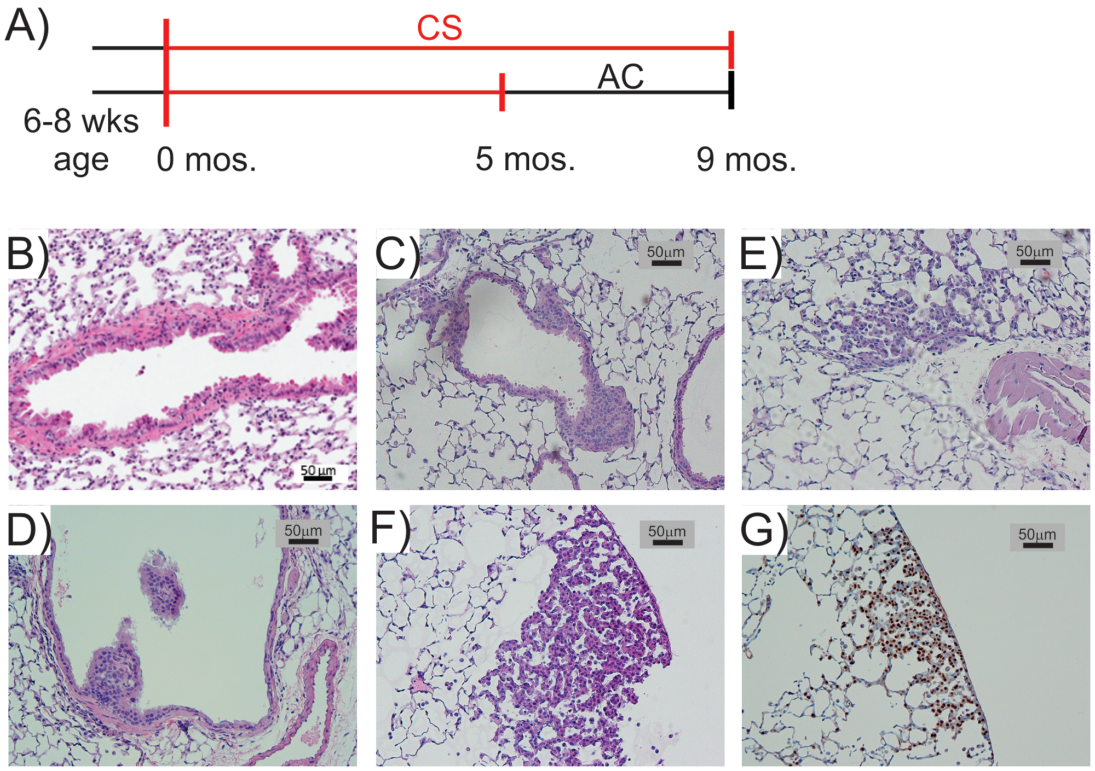

Figure 1. Morphology of CS exposed XPC-deficient and wild-type mice lungs. **(A)** Schematic of CS and AC exposed mice for the following morphologic evaluations. **(B)** Representative images of hematoxylin and eosin (H&E) stained lung epithelial cells showing precancerous changes including hyperplasia and atypia in an XPC-deficient (–/–) mouse exposed to 9 months of CS. XPC–/– mice exposed to 5 months CS followed by 4 months AC showed bronchiolar epithelial hyperplasia **(C, D)** with dysplasia **(D)**, early bronchioloalveolar adenoma **(E)** with adenocarcinoma *in situ* **(F)**. Immunohistochemical analysis (IHC) confirmed TTF1+ staining, consistent with adenocarcinoma-type histology **(G)**. ×200 magnification. Wks, weeks; Mos., months.

mouse models of CS exposure uniformly require chronic exposure to CS for several months followed by months of withdrawal from the exposure (27). In order to better align our cigarette smoking model to published models of lung cancer development in mice (28), we then exposed XPC+/+ and –/– mice to 5 months CS followed by 4 months of AC (Figure 1A). No tumors were observed on the lung surface by gross examination. On microscopic evaluation, both precancerous lesions and malignant tumors were observed only in XPC–/– mice. Precancerous changes included bronchiolar epithelial hyperplasia (Figure 1C), some with focal dysplastic features (Figure 1D). Other tumors showed histology characteristic of early bronchoalveolar carcinoma (Figure 1E) with some advancing to histologic characteristics similar to that observed in human adenocarcinoma *in situ* (Figure 1F and G).

Lung bronchoalveolar carcinomas typically arise from type 2 pneumocytes, found within the alveolar region of the lung. To further link impaired DNA repair to the increase in precancerous and malignant tumors observed in our smoking model, we evaluated the impact of XPC on DNA damage using type 2 pneumocytes from the lungs of XPC+/+ and –/– mice. High purity of type 2 pneumocyte isolation was confirmed by immunofluorescence microscopy for the type 2 pneumocyte-specific proteins, pro-SPC (Figures 2A and B). In primary murine type II alveolar cells, XPC expression protected against CSE-induced DNA damage as measured by alkaline comet assay ($P < 0.001$, Figure 2C). This further supports a role for XPC in protection against CS-induced DNA damage.

XPC deficiency increases urethane-induced lung adenocarcinoma

The murine CS-lung cancer model is a low-potency model for this strain of mouse (28). Given a signal of increased precancerous and malignant lung cancer development in XPC–/– mice in chronic CS, we further investigated the impact of XPC using a more robust urethane lung cancer carcinogen model.

Urethane is one of more than 7000 potentially carcinogenic compounds found in CS (4). On the basis of previous exposure models for C57BL/6 mice (21), littermate XPC+/+ and –/– mice aged 6–8 weeks were exposed to weekly urethane weekly for a total of 6 weeks and then evaluated for tumor development at 26 weeks (Figure 3A). Urethane exposure led to the development of grossly visible lung cancers in both XPC+/+ and –/– mice (Figure 3B). By visual inspection of the lung surface at the time of necropsy, XPC–/– mice averaged 17 times the number tumors compared with XPC+/+ ($P < 0.001$, Figure 3B and C). The tumors observed in the urethane-treated XPC–/– mice showed a range of histologic appearance and progression similar to the development of human adenocarcinoma by hematoxylin and eosin stain, ranging in histologic appearance from atypical adenomatous hyperplasia to adenoma to adenocarcinoma *in situ* and finally minimally invasive adenocarcinoma (Figure 3D, subpanels a–d). Adenocarcinoma histologic subtype was further supported by tumor positive TTF1 immunohistochemical analysis (Figure 3E). Treatment with urethane resulted in an increase in total BAL cell count, characterized as predominantly lymphocytes, in treated XPC–/– mice (Supplementary Figure 1A

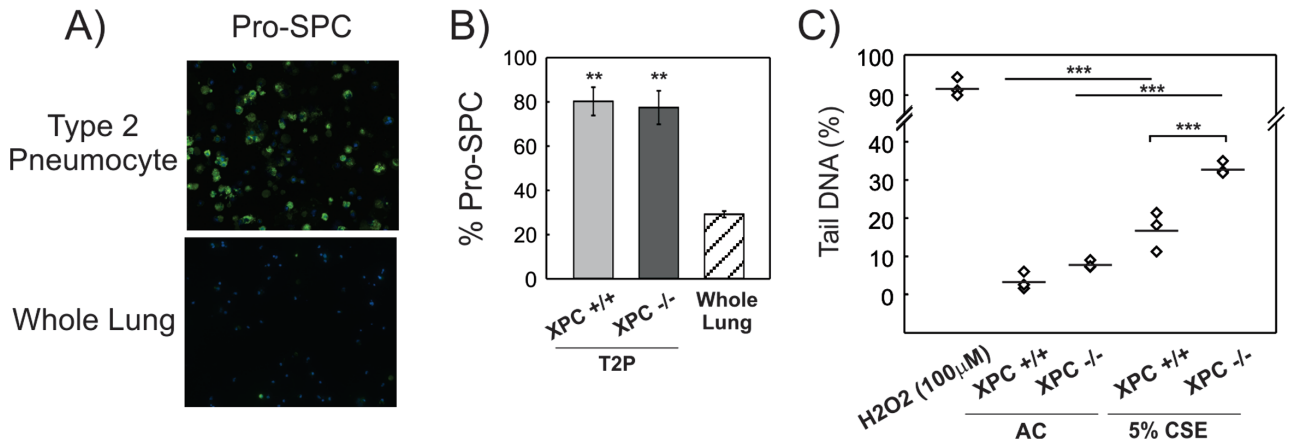

Figure 2. Impact of XPC on CS-induced DNA damage in type 2 pneumocytes. **(A)** Representative immunofluorescence microscopy image of pro-SPC staining in isolated type 2 pneumocytes compared with cells isolated from unselected lung cells (whole lung). Pro-SPC staining is shown in green, 4′,6-diamidino-2-phenylindole (DAPI) (nuclear) staining is shown in blue. ×200 magnification. **(B)** Mean percent type 2 pneumocytes (% pro-SPC) from the lungs of mice ($n = 3$) used in the subsequent experiment+/– standard error of the mean (SEM). Percent type 2 pneumocytes in whole lung isolate from XPC+/+ mice (shown for comparison) did not differ from that observed in whole lung isolate from XPC–/– mice (data not shown). $^{**}P < 0.01$ compared with whole lung. **(C)** Quantification of percentage of DNA in tail by alkaline comet assay in primary type II pneumocytes (XPC+/+ and XPC–/–) treated with AC or 5% CS extract CSE for 24 hours. Dots indicate the means of three independent experiments, each with ≥ 50 comets scored. Hydrogen peroxide (H2O2) shown as a positive (high DNA damage) control. $^{***}P < 0.001$.

and B, available at *Carcinogenesis* Online). Tumor number and size were not influenced by male or female sex, and tumor size was not affected by XPC expression (Supplementary Figure 1C and D, available at *Carcinogenesis* Online). Mice heterozygous for XPC (XPC+/–) developed an intermediate number of lung tumors with urethane exposure, averaging greater than twice the number of tumors compared with their XPC+/+ littermates (Figure 3F). These findings are highly suggestive of a protective effect of XPC against carcinogen exposure which may be dose-dependent.

XPC protects against urethane-induced lung cancers, in part through repair of oxidative DNA damage

We and others have suggested a role for XPC in repair of oxidative DNA lesions through the repair of oxidized DNA lesions through the BER pathway (11,15,20). The carcinogenic effects of urethane are believed to be related to the development of etheno adducts and oxidative lesions on DNA, both of which are repaired by the BER pathway (29,30). Lung tumors from XPC+/+ and –/– mice were stained for the oxidative DNA lesion, 8-OHdG. Strong immunohistochemical staining for 8-OHdG was observed in all lung tumors in both XPC+/+ and –/– mice (Figure 4A). To further investigate whether XPC protects against lung cancer development through repair of oxidative DNA damage, we provided mice with the antioxidant chemical, NAC (40 mM), in drinking water for 26 weeks (Figure 3A). Treatment with NAC resulted in a greater than 3-fold reduction in tumor number in XPC–/– mice compared with those treated with urethane alone ($P < 0.001$, Figure 4B) with no observed difference in tumor size (Supplementary Figure 2A, available at *Carcinogenesis* Online). The reduction in tumor number in XPC–/– mice treated with urethane + NAC was observed in both male and female mice (Supplementary Figure 2B, available at *Carcinogenesis* Online). However, death prior to scheduled necropsy was observed only in female XPC–/– mice receiving NAC (5/11 XPC–/– female mice receiving urethane + NAC compared with 0/12 XPC–/– mice receiving urethane alone) (Table 1). Interestingly, in those mice that survived to 26 weeks, no significant difference was observed in BAL cell count or differential in those mice receiving NAC in addition to urethane compared with those receiving urethane alone (Supplementary Figure 2C and D, available at *Carcinogenesis* Online).

To further define the mechanism by which XPC protects against CS-induced lung cancer development, we used another well-established murine model of lung adenocarcinoma development by exposing mice to the carcinogen MCA followed by BHT. XPC+/+ and –/– mice aged 6–8 weeks were exposed to one i.p. injection of MCA followed by 6 weekly i.p. injections of BHT (Figure 5A). At 24 weeks, there was a significant but modest increase in the number of tumors visible on the lung surface in XPC–/– mice when compared with +/+ mice, with XPC–/– mice treated with MCA-BHT developing twice the number of lung tumors as MCA-BHT-treated XPC+/+ mice (Figure 5B). Early malignant changes, corresponding in appearance to atypical adenomatous hyperplasia in humans, were observed in XPC+/+ mice treated with MCA-BHT. In XPC–/– mice treated with MCA-BHT, the tumors showed bronchoalveolar adenoma-type histology similar to human adenocarcinoma (Figure 5C and D), further confirmed by TTF-1 positive staining by immunohistochemical analysis (Figure 5E). As expected, an increase in BAL cell count and macrophages was observed in all mice treated with MCA-BHT but was independent of XPC genotype (Supplementary Figure 3, available at *Carcinogenesis* Online). These findings suggest that XPC repair of both oxidative and bulky (NER-repaired) DNA damage is probably involved in carcinogen-induced lung cancer development.

Discussion

In this study, we show that XPC plays an important role in CS carcinogen-induced lung cancer development. Using a murine model of CS exposure, we show that XPC deficiency accelerates precancerous changes and leads to development of a spectrum of murine lung bronchioloalveolar carcinomas with characteristics similar to human lung adenocarcinomas, ranging in histologic appearance from atypical adenomatous hyperplasia to adenoma to adenocarcinoma *in situ* and finally minimally invasive adenocarcinoma. A critical role of XPC in

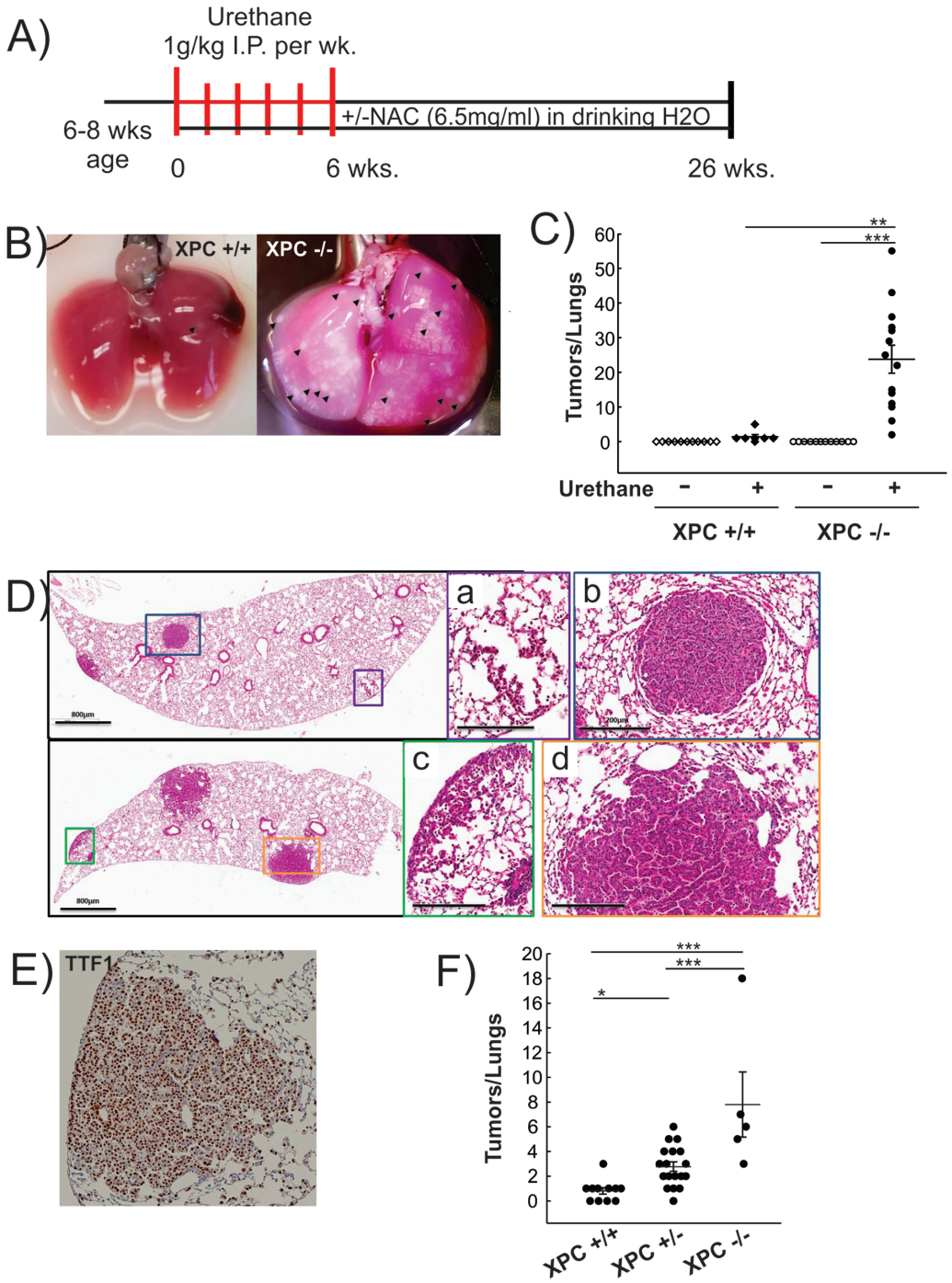

Figure 3. Impact of XPC on urethane-induced lung cancers. **(A)** Schematic of urethane experiments performed using XPC wild-type and deficient mice. **(B)** Representative gross images of lungs from XPC wild-type (+/+) and deficient (–/–) mice treated with urethane. Black arrow heads represent tumors visible on the lung surface. **(C)** Quantification of visible lung tumors in XPC+/+ and –/– mice treated with urethane. **(D)** Representative hematoxylin and eosin (H&E) of lungs from XPC-deficient mice showing progression of tumor from atypical adenomatous hyperplasia (a) to adenoma (b) to adenocarcinoma *in situ* (c) and minimally invasive adenocarcinoma (d) often within the same mouse. **(E)** Immunohistochemical analysis (IHC) confirmed TTF1+ staining, consistent with adenocarcinoma-type histology. **(F)** Quantification of visible lung tumors in XPC+/+, XPC heterozygous (+/–) and XPC–/– mice treated with urethane. *P < 0.05, **P < 0.01, ***P < 0.001.

CS carcinogen-related lung cancers is further supported by increased number of lung adenocarcinomas in XPC-deficient mice treated with two carcinogen models: urethane and MCA-BHT. These mouse models support a mechanism by which XPC deficiency leads to persistent DNA damage in XPC-deficient lung cells.

Carcinogen-induced DNA damage is believed to be the major driver of lung cancer development in smokers, with impaired DNA repair leading to mutations and ultimately cancer. However, how this occurs remains little understood. XPC has been implicated in lung cancer development. Several studies have proposed a link between common polymorphisms of XPC

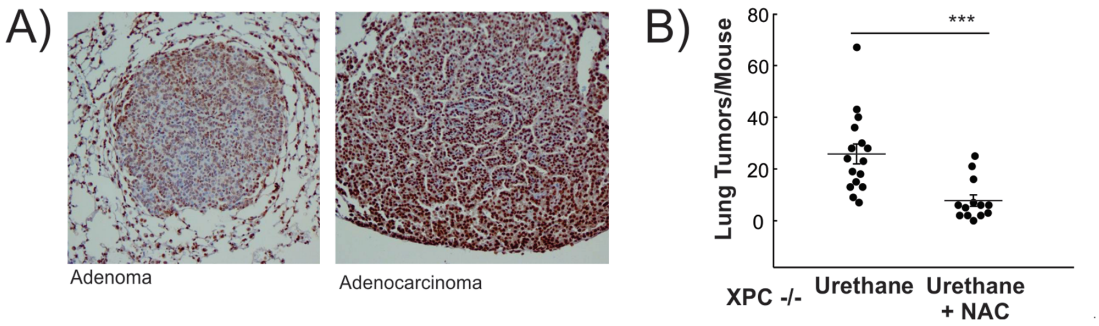

Figure 4. Impact of antioxidant treatment on urethane-induced lung cancer development in XPC-deficient mice **(A)** Immunohistochemical stain showing staining for 8-oxo-2′-deoxyguanosine (8-OHdG) in lower grade (adenoma, left) and higher grade (adenocarcinoma, right) tumors in the lung. **(B)** Quantification of lung tumors visible on the surface of mouse lungs in XPC-deficient (–/–) mice administered either drinking water or drinking water supplemented with NAC in addition to urethane. ***P < 0.001

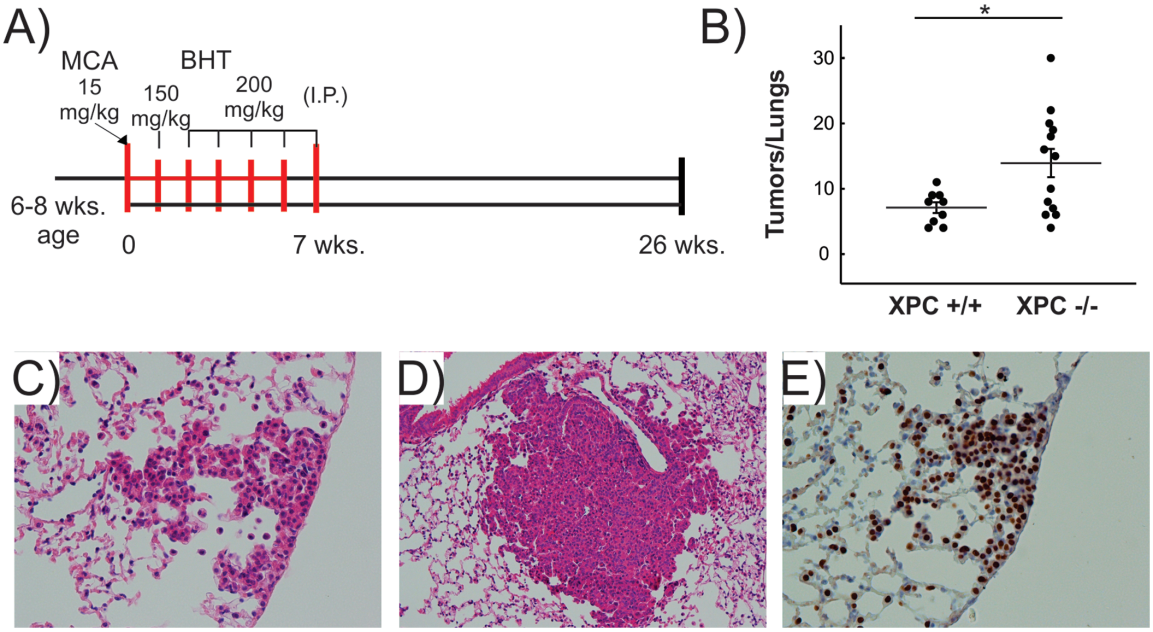

Figure 5. Impact of XPC on MCA-BHT-induced lung cancers. **(A)** Schematic of 3-methylcholanthrene-butylated hydroxytoluene (MCA-BHT) experiments performed using XPC wild-type and deficient mice. **(B)** Quantification of visible lung tumors in XPC+/+ and XPC–/– mice treated with MCA-BHT. **(C and D)** Representative hematoxylin and eosin stained sections of lung from XPC-deficient mice showing lung tumors of advancing adenocarcinoma histology. **(E)** Immunohistochemical analysis (IHC) confirmed TTF1+ staining, consistent with adenocarcinoma-type histology. *P < 0.05

and lung cancer development, although results have varied (31–34). XPC-deficient mice develop precancerous changes and adenomas with advanced age, and previous studies have suggested an important role for oxidative stress and oxidative DNA damage in cancer development (15). In Figure 1, we show a direct link between decreased XPC expression and CS- and carcinogen-induced lung cancer development in mice. XPC–/– mice showed acceleration of precancerous changes when exposed to chronic CS for 9 months and required withdrawal of CS (5 months of CS followed by 4 months of AC) for lung cancers to develop. This is not surprising, given that multiple studies support the requirements of an AC recovery period after CS for a murine model of lung cancer development (27). Of interest is that none of the XPC+/+ mice develop lung cancers after 5 months CS followed by 4 months of AC. We suspect this is due to a combination of the protective effects of XPC combined with a very low susceptibility of both the C57BL/6 and 129 mouse strains to induction of lung cancers by this method of chronic CS exposure, as has been observed previously (28).

Given the relatively low potency of the CS-lung cancer model in these mice, we turned to carcinogen lung adenocarcinoma models to evaluate the mechanism by which XPC protects against lung cancer development. As expected, we observed and increase in lung adenocarcinoma development in urethane-treated mice deficient in XPC when compared with their WT littermates (Figure 3). XPC+/– mice develop an intermediate number of lung tumors when treated with urethane compared with XPC–/– and XPC WT mice (Figure 4B), further supporting a mechanism by which the level of XPC expression contributes to development of CS carcinogen lung adenocarcinomas. Although XPC deficiency is rare, common polymorphisms or deletions of chromosome 3p, as commonly found in lung cancers (18,32,33,35), may result in intermediate levels of expression and/or function. Low XPC messenger RNA expression has also been associated with a shorter recurrence-free survival in 302 patients with resected NSCLC (36). Our finding that XPC+/– mice develop an intermediate number of lung tumors when treated with urethane suggests that loss of heterozygosity or

single XPC mutations, either through early malignant genomic changes or through genetic predisposition, may be sufficient for tumor development. The dose of urethane used in these studies is standard for development of adenocarcinoma in this mouse strain (21), however, one should use caution in directly correlating these results to CS-induced lung cancer, as the dose of urethane to which mice were exposed are much higher than that found in CS, and additional chemicals found in CS may impact of XPC on lung adenocarcinoma development as well.

This study shows a strong link between decreased DNA repair by XPC and lung cancer development in CS and carcinogen-exposed lung. We show that XPC is protective against CS-induced DNA damage in mouse primary type 2 pneumocytes, as measured by alkaline comet assay (Figure 2). XPC has a well-established role in GG-NER (13), however, this study also contributes to the growing understanding of the role of XPC in BER. It has been postulated that XPC aids in repair of oxidative DNA damage through BER, either by recognition of oxidative DNA lesions or through augmentation of nuclease activity, specifically of glycosylating proteins, hOgg1 and thymidine-DNA glycosylase (12–14). Urethane has been shown to cause DNA damage directly (etheno adducts) and indirectly through oxidative stress (development of oxidized bases or abasic intermediate sites) (30), both repaired primarily through BER. The increased tumor development in urethane-exposed XPC–/– mice and partial inhibition following the addition of NAC (Figures 3C and 4B) suggest that XPC-BER activity plays an important role in lung cancer development. However, this is not a direct mechanistic link and the incomplete inhibition of tumor development by NAC in XPC–/– mice might suggest a role for XPC–NER activity as well. Further supporting our finding of increased lung tumor development in XPC–/– mice treated with MCA-BHT (Figure 5). The synthetic carcinogen MCA is a PAH, which are repaired through the NER pathway (13). Supporting the importance of effective NER in protecting against lung cancer development are a number of studies showing a link between low NER activity in peripheral blood mononuclear cells and risk for lung cancer development (8). However, treatment with MCA alone leads to relatively modest numbers of lung tumors in mice, requiring treatment with the non-carcinogenic, proliferative agent BHT for aggressive lung cancer development (22). Considering reports of PAH induction of reactive oxygen species (37), this suggests an important role of XPC in both NER and BER for protection against lung cancer, probably with considerable overlap.

It is likely that other functions of XPC outside of its role in DNA repair are linked to lung cancer development. Decreased XPC expression leads to increased apoptosis and decreased clonogenic survival in CS-exposed bronchial epithelial cells, associated with accelerated emphysema development in XPC–/– mice (20). Similar findings of decreased clonogenic survival and altered cell cycle arrest were observed in XPC knockdown HeLa cells exposed to ultraviolet radiation *in vitro* (38). Interestingly, recent studies have suggested roles for XPC outside of its function in DNA damage recognition and repair. Increased proliferation, tumor growth and cell migration are seen in XPC knockdown NSCLC cells with decreased apoptosis observed DNA damaged skin keratinocytes deficient in XPC (39–41). It is likely that the impact of XPC on cell survival and proliferation are dependent on several factors impacting cell fate, including cell type, burden and type of DNA damage, and oncogene/tumor suppressor profiles. Further clarification of how XPC affects cellular function in response to CS and carcinogen exposure is important to further identify its role in lung cancer development. As the mice used in these experiments were globally deficient in XPC, we cannot fully rule out an effect of XPC on other processes including oxidative stress or local inflammation, both important to lung cancer development, as important in XPC CS-lung cancer development.

Mice treated with urethane developed few solid organ tumors other than lung (Table 1) with development of non-lethal lymphomas occurring equally in XPC+/+ and –/– mice, consistent with age-related strain susceptibility as previously observed (42). This supports prior murine studies which have shown a specificity of XPC deficiency to lung cancer development (14,18). It is not known whether XPC is unique in its protection against CS- and carcinogen-induced lung cancer development, as decreased NER activity has been implicated in a number of malignancies, including lung cancer (8,43), and relatively mild number of spontaneous tumors have been observed in mice deficient in the BER proteins hOgg1 and microtT homolog 1 (44). However, deficiency of another NER protein, XPA, led to increases in liver tumors and oxidant-induced mutations in the liver but no increase in lung tumor development (19). Further studies combining targeted knockdown of XPC and other DNA repair proteins with *in vitro* mechanistic studies are needed to further our understanding of the role of XPC and DNA repair in general in lung cancer development.

These studies present an intriguing role for XPC in lung cancer development and, along with our previous studies, suggest that XPC may play an important role against protecting against the two major smoking-related lung complications chronic obstructive pulmonary disease and lung cancer (20). Further defining the mechanisms by which XPC protects against CS-induced lung cancer may play an important role in prediction and prevention of lung cancer development in those exposed to CS and other carcinogens.

Supplementary material

Supplementary data are available at *Carcinogenesis* online.

Funding

American Cancer Society (128511-MRSG-15-163-01-DMC to C.R.S.); Showalter Research Foundation (to C.R.S.); Indiana CTSI (funded in part by National Institutes of Health-UL1 TR000006 to C.R.S).

Acknowledgements

We would like to thank members of Dr. John Turchi and Dr. Shadia Jalal's laboratories for critical review of the data and manuscript.
Conflict of Interest Statement: None declared.

References

1. Siegel, R.L. *et al.* (2015) Cancer statistics, 2015. CA. Cancer J. Clin., 65, 5–29.
2. Torre, L.A. *et al.* (2015) Global cancer statistics, 2012. CA. Cancer J. Clin., 65, 87–108.
3. American Cancer Society. (2014) Cancer Facts and Figures 2014. American Cancer Society, Atlanta.
4. Hang, B. (2010) Formation and repair of tobacco carcinogen-derived bulky DNA adducts. J. Nucleic Acids, 2010, 709521.
5. Zabarovsky, E.R. *et al.* (2002) Tumor suppressor genes on chromosome 3p involved in the pathogenesis of lung and other cancers. Oncogene, 21, 6915–6935.

6. Caramori, G. *et al.* (2011) Mechanisms involved in lung cancer development in COPD. Int. J. Biochem. Cell Biol., 43, 1030–1044.
7. Hanahan, D. *et al.* (2011) Hallmarks of cancer: the next generation. Cell, 144, 646–674.
8. Shen, H. *et al.* (2003) Smoking, DNA repair capacity and risk of nonsmall cell lung cancer. Int. J. Cancer, 107, 84–88.
9. Trego, K.S. *et al.* (2006) Pre-steady-state binding of damaged DNA by XPC-hHR23B reveals a kinetic mechanism for damage discrimination. Biochemistry, 45, 1961–1969.
10. Guo, C. *et al.* (2010) SnapShot: nucleotide excision repair. Cell, 140, 754–4.e1.
11. D'Errico, M. *et al.* (2006) New functions of XPC in the protection of human skin cells from oxidative damage. EMBO J., 25, 4305–4315.
12. Shimizu, Y. *et al.* (2003) Xeroderma pigmentosum group C protein interacts physically and functionally with thymine DNA glycosylase. EMBO J., 22, 164–173.
13. Sugasawa, K. (2008) XPC: its product and biological roles. In Ahmad, S. and Hanaoka, F. (eds) Molecular Mechanisms of Xeroderma Pigmentosum. Landes Bioscience and Springer Science+Business Media, New York, pp. 47–56.
14. Melis, J.P. *et al.* (2011) The role of XPC: implications in cancer and oxidative DNA damage. Mutat. Res., 728, 107–117.
15. Melis, J.P. *et al.* (2013) Slow accumulation of mutations in Xpc–/– mice upon induction of oxidative stress. DNA Repair (Amst), 12, 1081–1086.
16. DiGiovanna, J.J. *et al.* (2012) Shining a light on xeroderma pigmentosum. J. Invest. Dermatol., 132(Pt 2), 785–796.
17. Qiu, L. *et al.* (2008) Associations between XPC polymorphisms and risk of cancers: a meta-analysis. Eur. J. Cancer, 44, 2241–2253.
18. Hollander, M.C. *et al.* (2005) Deletion of XPC leads to lung tumors in mice and is associated with early events in human lung carcinogenesis. Proc. Natl. Acad. Sci. USA, 102, 13200–13205.
19. Melis, J.P. *et al.* (2008) Mouse models for xeroderma pigmentosum group A and group C show divergent cancer phenotypes. Cancer Res., 68, 1347–1353.
20. Sears, C.R. *et al.* (2018) Xeroderma pigmentosum group C deficiency alters cigarette smoke DNA damage cell fate and accelerates emphysema development. Am. J. Respir. Cell Mol. Biol., 58, 402–411.
21. Miller, Y.E. *et al.* (2003) Induction of a high incidence of lung tumors in C57BL/6 mice with multiple ethyl carbamate injections. Cancer Lett., 198, 139–144.
22. Fritz, J.M. *et al.* (2010) The Kras mutational spectra of chemically induced lung tumors in different inbred mice mimics the spectra of KRAS mutations in adenocarcinomas in smokers versus nonsmokers. J. Thorac. Oncol., 5, 254–257.
23. D'Agostini, F. *et al.* (2000) Interactions between N-acetylcysteine and ascorbic acid in modulating mutagenesis and carcinogenesis. Int. J. Cancer, 88, 702–707.
24. Rice, W.R. *et al.* (2002) Maintenance of the mouse type II cell phenotype *in vitro*. Am. J. Physiol. Lung Cell. Mol. Physiol., 283, L256–L264.
25. Sears, C.R. *et al.* (2016) DNA damage response (DDR) pathway engagement in cisplatin radiosensitization of non-small cell lung cancer. DNA Repair (Amst), 40, 35–46.
26. Olive, P.L. *et al.* (2006) The comet assay: a method to measure DNA damage in individual cells. Nat. Protoc., 1, 23–29.
27. Witschi, H. *et al.* (1997) The carcinogenicity of environmental tobacco smoke. Carcinogenesis, 18, 575–586.
28. Gordon, T. *et al.* (2009) Strain-dependent differences in susceptibility to lung cancer in inbred mice exposed to mainstream cigarette smoke. Cancer Lett., 275, 213–220.
29. Sakano, K. *et al.* (2002) Metabolism of carcinogenic urethane to nitric oxide is involved in oxidative DNA damage. Free Radic. Biol. Med., 33, 703–714.
30. Guengerich, F.P. *et al.* (1991) Enzymatic oxidation of ethyl carbamate to vinyl carbamate and its role as an intermediate in the formation of 1,N6-ethenoadenosine. Chem. Res. Toxicol., 4, 413–421.
31. Jin, B. *et al.* (2014) Association of XPC polymorphisms and lung cancer risk: a meta-analysis. PLoS One, 9, e93937.
32. Francisco, G. *et al.* (2008) XPC polymorphisms play a role in tissue-specific carcinogenesis: a meta-analysis. Eur. J. Hum. Genet., 16, 724–734.
33. Huang, W.Y. *et al.* (2006) Nucleotide excision repair gene polymorphisms and risk of advanced colorectal adenoma: XPC polymorphisms modify smoking-related risk. Cancer Epidemiol. Biomarkers Prev., 15, 306–311.
34. Marín, M.S. *et al.* (2004) Poly (AT) polymorphism in intron 11 of the XPC DNA repair gene enhances the risk of lung cancer. Cancer Epidemiol. Biomarkers Prev., 13(Pt 1), 1788–1793.
35. Qiao, B. *et al.* (2011) *In vitro* functional effects of XPC gene rare variants from bladder cancer patients. Carcinogenesis, 32, 516–521.
36. Yeh, K.T. *et al.* (2012) XPC mRNA level may predict relapse in never-smokers with non-small cell lung cancers. Ann. Surg. Oncol., 19, 734–742.
37. Munoz, B. *et al.* (2011) DNA damage caused by polycyclic aromatic hydrocarbons: mechanisms and markers. In Chen, C. (ed) Selected Topics in DNA Repair. InTech, pp. 125–144. http://www.intechopen.com/books/selected-topics-in-dna-repair/dna-damage-causedby-polycyclic-aromatic-hydrocarbons-mechanisms-and-markers. (26 September 2017, date last accessed).
38. Renaud, E. *et al.* (2011) Differential contribution of XPC, RAD23A, RAD23B and CENTRIN 2 to the UV-response in human cells. DNA Repair (Amst), 10, 835–847.
39. Cui, T. *et al.* (2015) XPC inhibits NSCLC cell proliferation and migration by enhancing E-Cadherin expression. Oncotarget, 6, 10060–10072.
40. Wang, Q.E. *et al.* (2012) Nucleotide excision repair factor XPC enhances DNA damage-induced apoptosis by downregulating the antiapoptotic short isoform of caspase-2. Cancer Res., 72, 666–675.
41. Sun, C.C. *et al.* (2016) MicroRNA-346 facilitates cell growth and metastasis, and suppresses cell apoptosis in human non-small cell lung cancer by regulation of XPC/ERK/Snail/E-cadherin pathway. Aging (Albany. NY), 8, 2509–2524.
42. Smith, G.S. *et al.* (1973) Lifespan and incidence of cancer and other diseases in selected long-lived inbred mice and their F 1 hybrids. J. Natl. Cancer Inst., 50, 1195–1213.
43. Wei, Q. *et al.* (1997) The role of DNA repair capacity in susceptibility to lung cancer: a review. Cancer Metastasis Rev., 16, 295–307.
44. Paz-Elizur, T. *et al.* (2003) DNA repair activity for oxidative damage and risk of lung cancer. J. Natl. Cancer Inst., 95, 1312–1319.